



Contents lists available at SciVerse ScienceDirect

# Spectrochimica Acta Part A: Molecular and Biomolecular Spectroscopy

journal homepage: [www.elsevier.com/locate/saa](http://www.elsevier.com/locate/saa)

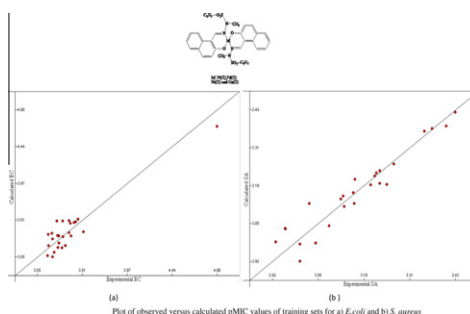
## Synthesis, characterization and anti-microbial evaluation of Cu(II), Ni(II), Pt(II) and Pd(II) sulfonylhydrazone complexes; 2D-QSAR analysis of Ni(II) complexes of sulfonylhydrazone derivatives

Neslihan Özbek<sup>a,\*</sup>, Saliha Alyar<sup>b</sup>, Hamit Alyar<sup>c</sup>, Ertan Şahin<sup>d</sup>, Nurcan Karacan<sup>e</sup><sup>a</sup> Department of Primary Education, Faculty of Education, Ahi Evran University, TR-40100 Kırşehir, Turkey<sup>b</sup> Department of Chemistry, Science and Art Faculty, Karatekin University, TR-18100 Çankırı, Turkey<sup>c</sup> Department of Physics, Science and Art Faculty Karatekin University, TR-18100 Çankırı, Turkey<sup>d</sup> Department of Chemistry, Faculty of Science, Atatürk University, TR-25240 Erzurum, Turkey<sup>e</sup> Department of Chemistry, Faculty of Science and Art, Gazi University, TR-06500 Ankara, Turkey

### HIGHLIGHTS

- ▶ New original sulfonylhydrazine and sulfonylhydrazone complexes were synthesized.
- ▶ New synthesized compounds were screened for their antibacterial activity.
- ▶ QSAR analysis was performed on Ni(II) sulfonylhydrazone complexes for *E. coli* and *S. aureus*.

### GRAPHICAL ABSTRACT

Plot of observed versus calculated pMIC values of training sets for: (a) *E. coli* and (b) *S. aureus*

### ARTICLE INFO

#### Article history:

Received 19 October 2012

Received in revised form 17 December 2012

Accepted 5 January 2013

Available online 26 January 2013

#### Keywords:

Sulfonylhydrazide

Sulfonylhydrazone

X-ray structure

Antimicrobial activity

2D-QSAR

Ni(II) sulfonyl hydrazone derivatives

### ABSTRACT

Copper(II), nickel(II), platinum(II) and palladium(II) complexes with 2-hydroxy-1-naphthaldehyde-N-methylpropanesulfonylhydrazone (*nafpsmh*) derived from propanesulfonic acid-1-methylhydrazide (*psmh*) were synthesized, their structure were identified, and antimicrobial activity of the compounds was screened against three Gram-positive and three Gram-negative bacteria. The results of antimicrobial studies indicate that Pt(II) and Pd(II) complexes showed the most activity against all bacteria. The crystal structure of 2-hydroxy-1-naphthaldehyde-N-methylpropanesulfonylhydrazone (*nafpsmh*) was also investigated by X-ray analysis. A series of Ni(II) sulfonyl hydrazone complexes (1–33) was synthesized and tested in vitro against *Escherichia coli* and *Staphylococcus aureus*. Their antimicrobial activities were used in the QSAR analysis. Four-parameter QSAR models revealed that nucleophilic reaction index for Ni and O atoms, and HOMO–LUMO energy gap play key roles in the antimicrobial activity.

© 2013 Elsevier B.V. All rights reserved.

### Introduction

Sulfa drugs are considered to be among the most important group of compounds in medicinal chemistry due to their preparative accessibility, structural variety and wide biological profile

\* Corresponding author.

E-mail address: [nozбек@ahievran.edu.tr](mailto:nozбек@ahievran.edu.tr) (N. Özbek).

[1,2], such as antibacterial [3], antitumor [4,5], anti-carbonic anhydrase [6–8], diuretic [9], hypoglycemic [10], anti-thyroid [11], protease inhibitor [12] and anticonvulsant [7] activities. The growing anti-microbial drug resistance, particularly the emergence of multi-drug resistant strains of Gram-positive bacteria pathogens such as *Staphylococcus aureus*, is a problem of increasing significance. One way to counterbalance this problem is to develop novel anti-

microbial agents. Consequently, the search for new anti-microbial agents will always remain of importance for medicinal chemists.

The literature review reveals that sulfonyl hydrazone and sulfonyl hydrazide derivatives have wide spectrum of antimicrobial [13–18], antifungal [19] and anticytotoxic [20] activities. Keeping this observation in mind, in continuation of our study [21–25] 2-hydroxy-1-naphthaldehyde-*N*-methylpropanesulfonylhydrazone (*nafpsmh*) derived from propanesulfonic acid 1-methylhydrazide (*psmh*), and copper(II), nickel(II), platinum(II), palladium(II) complexes of *nafpsmh* were synthesized, and their structures were identified by spectrochemical techniques, magnetic susceptibility, conductivity measurement and elemental analysis. These compounds were tested against three Gram-negative (*Escherichia coli* ATCC 25922, *Pseudomonas aeruginosa* ATCC 27853 and *Yersinia enterocolitica* 0:3) and three Gram-positive (*Bacillus subtilis* ATCC 6633, *S. aureus* ATCC 25923 and *Bacillus cereus* RSKK 709) bacterial strains by using the microdilution broth and disc diffusion methods.

Several in silico techniques are utilized in the process of drug design. One such technique is quantitative structure–activity relationship (QSAR). QSAR is a quantitative correlation between physicochemical parameters of chemical structure and their biological activity [26–29]. This method has been utilizing to improve the structure of compounds and to interpret the structures in terms of biological interactions [30–32].

We have already reported a quantitative structure–activity relationship study on anti-bacterial agents for disulfonamide [33]. Continuing this effort, herein we performed a quantitative structure–activity relationship study of Ni(II) sulfonyl hydrazone complexes as anti-bacterial agents against *E. coli* and *S. aureus*.

## Experimental

### Physical measurements

The crystal structure of 2-Hydroxy-1-naphthaldehyde-*N*-methylpropanesulfonylhydrazone (*nafpsmh*) was determined by using a four-circle Rigaku R-AXIS RAPID-S diffractometer equipped with a two-dimensional area IP detector. The elemental analyses (C, H, N and S) were performed on a LECO-CHSNO-9320 type elemental analyzer. The IR spectra (4000–400 cm<sup>-1</sup>) were recorded on a Mattson-1000 FT-IR spectrophotometer with samples prepared as KBr pellets. NMR spectra were recorded on a Bruker-Spectrospin Avance DPX – 400 Ultra – Shield (400 MHz) by using DMSO as a solvent and TMS as an internal standard. LC/MS-APCI was recorded on AGILENT 1100. The melting point was recorded on Opti Melt apparatus. TLC was conducted on 0.25 mm silica gel plates (60F254, Merck). Visualization was made by using ultraviolet light. All extracted solvents (all from Merck) were dried over anhydrous Na<sub>2</sub>SO<sub>4</sub> and evaporated by using a BUCHI rotary evaporator. Reagents were obtained commercially from Aldrich (ACS grade) and used without purification. Melting points of the compounds were determined with a Gallenkamp melting point apparatus. The molar magnetic susceptibilities were measured on powdered samples using the Gouy method. The molar conductance measurements were carried out using a Siemens WPA CM 35 conductometer.

### Synthesis

General synthesis method of the compounds was depicted schematically in Fig. 1.

#### Propanesulfonic acid 1-methylhydrazide (*psmh*)

Propanesulfonyl chloride (0.05 mol) in tetrahydrofuran (30 mL) was added to methylhydrazine (0.08 mol) dropwise while the temperature was maintained between 268 and 273 K. The mixture was

stirred for 24 h (completion of the reaction was monitored by TLC), then the solvent was evaporated. The colorless crude compound was purified in THF/n-hexane by column chromatography, and then the product was crystallized from the THF/n-hexane mixture (2:1). Yield 72%; mp: 115–117 °C, EI-MS (70 eV) *m/z*: 214.12 (2M<sup>+</sup>, 10.2%), 200.2 (2M<sup>+</sup>–CH<sub>3</sub>, 18.7%), Elemental analysis: Calcd. for C<sub>4</sub>H<sub>12</sub>SO<sub>2</sub>N<sub>2</sub>: C, 31.56; H, 7.947; N, 18.4 S, 21.06. Found: C, 31.81; H, 8.03; N, 17.91; S, 20.84.

#### 2-Hydroxy-1-naphthaldehyde-*N*-methylpropanesulfonylhydrazone (*nafpsmh*)

Ethanol/ethyl acetate (1:1) solution of propanesulfonic acid 1-methylhydrazide (0.5 g, 3.29 mmole) was added drop wise to an ethanol/ethyl acetate (1:1) solution of 2-hydroxy-1-naphthaldehyde (0.736 g, 4.2 mmole), maintaining the temperature at about 323 K. Then, the mixture was stirred for 24 h at room temperature. The precipitated product was crystallized from the ethanol/n-hexane (3:1) mixture. The yellow crystalline solid was dried in vacuum and stored in ethanol/n-hexane vapor. Yield 65%; mp: 164–166 °C, EI-MS (70 eV) *m/z*: 306.9 (M<sup>+</sup>, 9.6%), 200.1 (M<sup>+</sup>–C<sub>3</sub>H<sub>7</sub>SO<sub>2</sub>, 18.7%), Elemental analysis: Anal. Calcd. for C<sub>15</sub>H<sub>18</sub>SO<sub>3</sub>N<sub>2</sub>: C, 58.8; H, 5.921; N, 9.143; S, 10.465. Found: C, 59.04; H, 5.74; N, 9.22; S, 10.5.

#### Synthesis of Cu(II) complex; Cu(*nafpsmh*)<sub>2</sub>

A copper(II) chloride (0.067 g, 0.5 mmole) and sodium hydroxide solution was added slowly to a sample of anhydrous acetonitrile (20 mL) of 2-hydroxy-1-naphthaldehyde-*N*-methylpropanesulfonylhydrazone (0.307 g, 1.0 mmole). The reaction mixture was heated at 313 K for 2 h. The mixture was stirred for 24 h, the resulting brown powder was filtrated and washed with a small volume of dimethylformamide, and then dried in a desiccator over CaCl<sub>2</sub>. Yield 65%; mp: 222–224 °C, EI-MS (70 eV) *m/z*: 674.85 (M<sup>+</sup>, 11.5%), 305.8 (C<sub>15</sub>H<sub>17</sub>SO<sub>3</sub>N<sub>2</sub><sup>+</sup>, 100%), Elemental analysis: Anal. Calcd. for C<sub>30</sub>H<sub>34</sub>S<sub>2</sub>O<sub>6</sub>N<sub>4</sub>Cu: C, 53.44; H, 5.08; N, .831; S, 9.51. Found: C, 55.04; H, 5.62; N, 8.81; S, 9.1.

#### Synthesis of Ni(II) complex; Ni(*nafpsmh*)<sub>2</sub>

A nickel(II) chloride (0.065 g; 0.505 mmole) and sodium hydroxide solution was added slowly to a sample of anhydrous acetonitrile (20 mL) of 2-hydroxy-1-naphthaldehyde-*N*-methylpropanesulfonylhydrazone (0.311 g, 1.01 mmole). The reaction mixture was heated at 313 K for 2 h. The mixture was stirred for 24 h, the resulting green powder was filtrated and washed with a small volume of ether, and then dried in a desiccator over CaCl<sub>2</sub>. Yield 84%; mp: 244–245 °C, EI-MS (70 eV) *m/z*: 670.2 (M<sup>+</sup>, 13.6%), 305.6 (C<sub>15</sub>H<sub>17</sub>SO<sub>3</sub>N<sub>2</sub><sup>+</sup>, 100%), Elemental analysis: Anal. Calcd. for C<sub>30</sub>H<sub>34</sub>S<sub>2</sub>O<sub>6</sub>N<sub>4</sub>Ni: C, 53.83; H, 5.12; N, .837; S, 9.58. Found: C, 54.2; H, 5.32; N, 8.46; S, 9.9.

#### Synthesis of Pt(II) complex; Pt(*nafpsmh*)<sub>2</sub>

A platinum(II) chloride (0.139 g; 0.52 mmole) and sodium hydroxide solution in methanol was added slowly to a sample of anhydrous acetonitrile solution of 2-hydroxy-1-naphthaldehyde-*N*-methylpropanesulfonylhydrazone (0.322 g, 1.04 mmole). The reaction mixture was heated at 333 K for 3 h. The mixture was stirred for two days, the resulting dark green powder was filtrated and washed with a small volume of ether, and then dried in a desiccator over CaCl<sub>2</sub>. Yield 72%; mp: 264–267 °C, EI-MS (70 eV) *m/z*: 806.3 (M<sup>+</sup>, 14.4%), 305.9 (C<sub>15</sub>H<sub>17</sub>SO<sub>3</sub>N<sub>2</sub><sup>+</sup>, 100%), Elemental analysis: Anal. Calcd. for C<sub>30</sub>H<sub>34</sub>S<sub>2</sub>O<sub>6</sub>N<sub>4</sub>Pt: C, 44.71; H, 4.25; N, .695; S, 7.96. Found: C, 44.30; H, 4.74; N, 7.05; S, 8.22.

#### Synthesis of Pd(II) complex; Pd(*nafpsmh*)<sub>2</sub>

A palladium(II) chloride (0.097 g; 0.54 mmole) and sodium hydroxide solution in methanol was added slowly to a sample of anhydrous acetonitrile of 2-hydroxy-1-naphthaldehyde-*N*-meth-

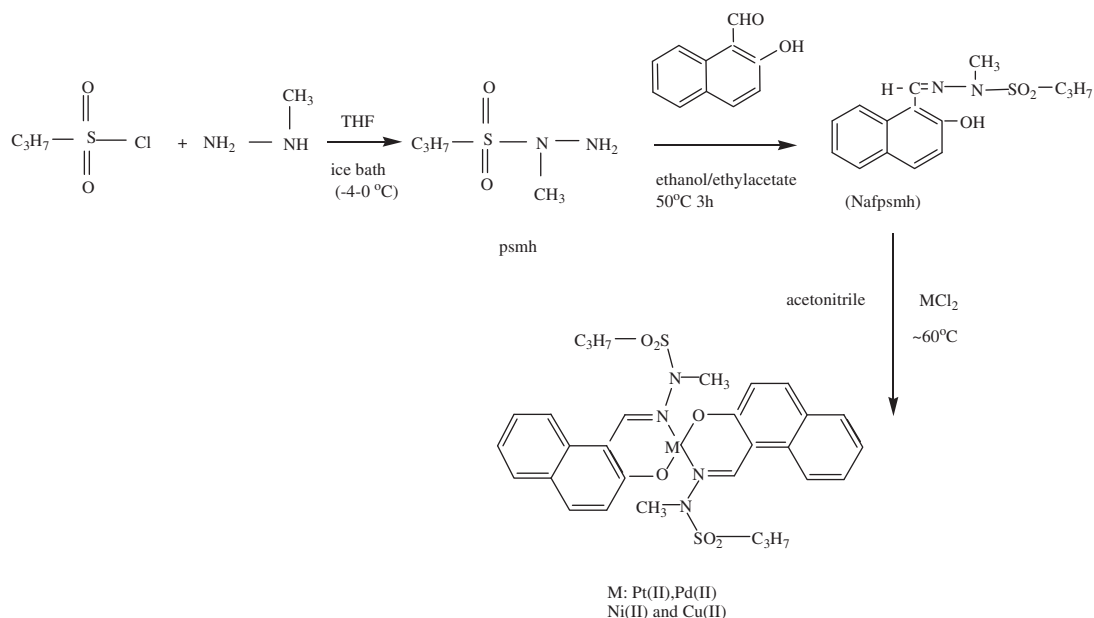


Fig. 1. General synthetic scheme of our compounds.

ylpropanesulfonylhydrazone (0.335 g, 1.09 mmole). The reaction mixture was heated at 333 K for 3 h. The mixture was stirred for two days, the resulting orange powder was filtrated and washed with a small volume of ether, and then dried in a desiccator over  $\text{CaCl}_2$ . Yield 60%; mp: 280–284 °C. EI-MS (70 eV)  $m/z$ : 718.2 ( $\text{M}^+$ , 13.5%), 305.7 ( $\text{C}_{15}\text{H}_{17}\text{SO}_3\text{N}_2^+$ , 100%), Elemental analysis: Anal. Calcd. for  $\text{C}_{30}\text{H}_{34}\text{S}_2\text{O}_6\text{N}_4\text{Pd}$ : C, 50.24; H, 4.78; N, 7.81; S, 8.94 Found: C, 50.02; H, 4.46; N, 8.06; S, 9.11.

#### Crystal structure determination

For the crystal structure determination, the single-crystal of the compound *nafpsmh* was used for data collection on a four-circle Rigaku RAXIS RAPID-S diffractometer equipped with a two-dimensional area IP detector. The graphite-monochromatized Mo  $K\alpha$  radiation ( $\lambda = 0.71073 \text{ \AA}$ ) and oscillation scans techniques with  $\Delta\omega = 5^\circ$  for one image were used for data collection. Images were successfully taken by varying  $\omega$  with three sets of different  $\chi$  and  $\varphi$  values. The lattice parameters were determined by the least-squares method on the basis of all reflections with  $F^2 > 2\sigma(F^2)$ . Integration of the intensities, correction for Lorentz and polarization effects, and cell refinement were performed using CRYSTAL CLEAR (Rigaku/MSI Inc., 2005) software [34]. The structures were solved by the direct method using SHELXS. The positional and atomic displacement parameters (ADPs) were refined by the full-matrix least-squares method using SHELXL [35]. The positional and isotropic atomic displacement parameters of hydrogen atoms were refined together with other structural parameters by the full-matrix least-squares procedure based on the squared value of the structure factors. Hydrogen positions were calculated from assumed geometries and O–H hydrogen atom that was located on the difference map. H-atoms were included in structure factor calculations, but they were not refined. The isotropic displacement parameters of the hydrogen atoms were approximated from the  $U(\text{eq})$  value of the atom to which they were bonded. The final difference Fourier maps showed no peaks of chemical significance. Details of the X-ray data collection, structure solution and structure refinements are given in Table 1. Selected bond distances and angles are listed in Table 2. Intramolecular hydrogen bond present in the *nafpsmh* is given Table 3. The molecular structure with the atom-numbering schema is shown in Fig. 2a.

#### Antimicrobial activity

*E. coli* ATCC 35218, *P. aeruginosa* ATCC 27853, *Y. enterocolitica* 0:3, *B. subtilis* ATCC6633, *S. aureus* ATCC 25923 and *B. cereus* RSKK 709 cultures were obtained from Gazi University, Biology Department. Bacterial strains were cultured overnight at 37 °C in Nutrient Broth. During the survey, these stock cultures were stored in the dark at 4 °C.

#### Disc diffusion method

The synthesized compounds and complexes were dissolved in dimethylsulfoxide (20% DMSO) to a final concentration of  $10 \text{ mg mL}^{-1}$  and sterilized by filtration by  $0.45 \mu\text{m}$  Millipore filters. Antimicrobial tests were then carried out by the disc diffusion method using  $100 \mu\text{L}$  of suspension containing  $10^8 \text{ CFU mL}^{-1}$  bac-

Table 1  
Crystal data and details of structure refinement for the *nafpsmh*.

Empirical formula	$\text{C}_{15}\text{H}_{18}\text{SO}_3\text{N}_2$
$M_r$	306.4
$T$ (K)	293
Radiation, $\lambda$ (Å)	0.71073
Crystal system	Monoclinic
Space group	$P2_1/n$
Unit cell dimensions	
$a$ (Å)	6.0685(5)
$b$ (Å)	24.0493(13)
$c$ (Å)	10.5861(11)
Cell angle	$\alpha = 90.00$ , $\beta = 99.61(5)$ , $\gamma = 90.00$
$V$ (Å <sup>3</sup> )	1523.3(2)
$Z$	4
$D_c$ (g/cm <sup>3</sup> )	1.34
$\mu$ (mm <sup>-1</sup> )	0.224
$F(000)$	648
Crystal size (mm)	$0.28 \times 0.12 \times 0.07$
$\theta$ -range (°)	2.1 and 26.4
Index ranges ( $h, k, l$ )	$-7 \leq h \leq 7$ , $-30 \leq k \leq 30$ $-13 \leq l \leq 13$
Reflections collected	31963
Independent reflections ( $R_{\text{int}}$ )	3125(0.101)
Absorption correction	Multiscan
Goodness-of-fit on $F^2$	1.000
Final $R$ indices [ $I > 2\sigma(I)$ ]	0.074
$wR$ indices (all data)	0.165
Largest diff. peak and hole (e Å <sup>-3</sup> )	0.344 and $-0.303$

**Table 2**  
Selected bond distances (Å) and angles (°) for *nafpsmh*.

S—O(3)	1.427(4)	S—O(2)	1.437(4)
S—N(2)	1.653(4)	S—C(13)	1.765(6)
O(1)—H(1)	0.820(4)	O(1)—C(8)	1.339(6)
N(1)—N(2)	1.379(5)	N(1)—C(11)	1.283(6)
N(2)—C(12)	1.461(6)	C(8)—C(7)	1.405(7)
O(3)—S—O(2)	118.9(3)	O(3)—S—N(2)	106.1(2)
O(3)—S—C(13)	111.9(3)	O(2)—S—N(2)	106.8(2)
O(2)—S—C(13)	104.8(3)	N(2)—S—C(13)	107.8(3)
H(1)—O(1)—C(8)	109.5(4)	N(2)—N(1)—C(11)	120.0(4)
S—N(2)—N(1)	111.0(3)	S—N(2)—C(12)	122.4(3)
N(1)—N(2)—C(12)	122.4(4)	O(1)—C(8)—C(7)	123.6(4)

**Table 3**  
Intramolecular hydrogen bond present in *nafpsmh* (Å and °).

D—H...A	d(H...A)	d(D...A)	<(DHA)
O(1)—H...N(1)	1.85	2.563(5)	145

teria spread on a nutrient agar (NA) medium. The discs (6 mm in diameter) were impregnated with 20  $\mu\text{L}$  of each compound (200  $\mu\text{g}/\text{disc}$ ) at the concentration of 10  $\text{mg mL}^{-1}$  and placed on the inoculated agar. DMSO impregnated discs were used as negative control. Ciprofloxacin (5  $\mu\text{g}/\text{disc}$ ) and Ampicillin (10  $\mu\text{g}/\text{disc}$ ) were used as positive reference standards to determine the sensitivity of one strain/isolate in each microbial species tested. The inoculated plates were incubated at 37 °C for 24 h for bacterial strains isolates. Antimicrobial activity in the disc diffusion assay was evaluated by measuring the zone of inhibition against the test organisms. Each assay in this experiment was repeated twice [36].

#### Microdilution assays

The minimal inhibition concentration (MIC) values, except one, were also studied for the microorganisms sensitive to at least one of the five compounds determined in the disc diffusion assay. The inocula of microorganisms were prepared from 12 h broth cultures and suspensions were adjusted to 0.5 McFarland standard turbidity. The test compounds dissolved in dimethylsulfoxide (DMSO) were first diluted to the highest concentration (2400  $\mu\text{g mL}^{-1}$ ) to

be tested, and then serial, twofold dilutions were made in a concentration range from 18.75 to 2400  $\mu\text{g mL}^{-1}$  in 10 mL sterile test tubes containing nutrient broth. The MIC values of each compound against bacterial strains were determined based on a micro-well dilution method [37]. The 96-well plates were prepared by dispensing 95  $\mu\text{L}$  of nutrient broth and 5  $\mu\text{L}$  of the inoculum into each well. One hundred  $\mu\text{L}$  from each of the test compounds initially prepared at the concentration of 2400  $\mu\text{g mL}^{-1}$  was added into the first wells. Then, 100  $\mu\text{L}$  from each of their serial dilutions was transferred into eight consecutive wells. The last well containing 195  $\mu\text{L}$  of nutrient broth without compound, and 5  $\mu\text{L}$  of the inoculum on each strip, was used as negative control. The final volume in each well was 200  $\mu\text{L}$ . The contents of the wells were mixed and the microplates were incubated at 37 °C for 24 h. All compounds tested in this study were screened twice against each microorganism. The MIC was defined as the lowest concentration of the compounds to inhibit the growth of microorganisms.

#### Theoretical calculations and QSAR analysis

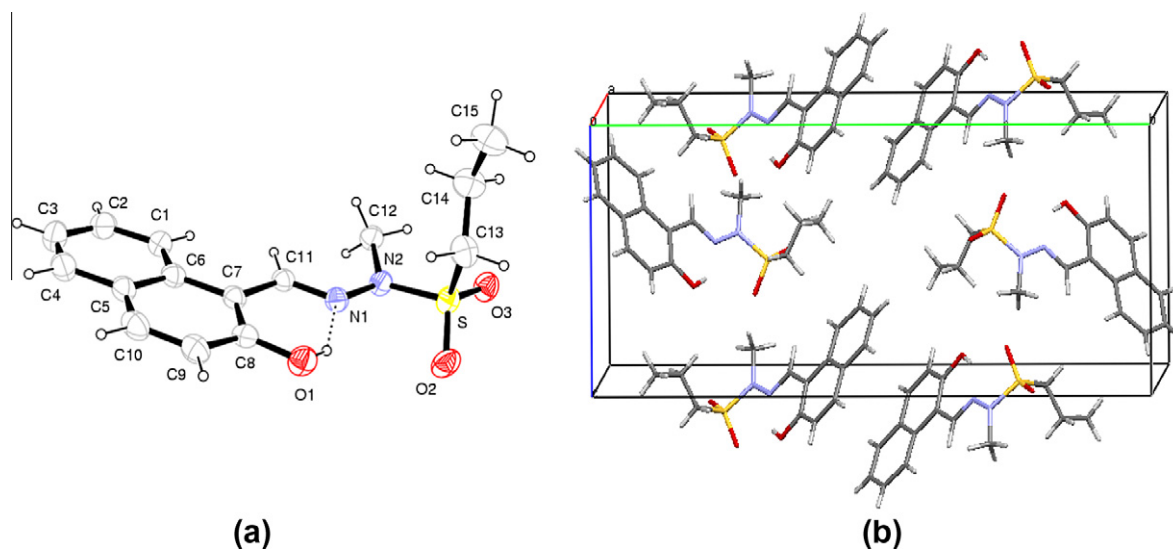
The molecular geometry optimizations of *propanesulfonic acid 1-methylhydrazide* and *2-hydroxy-1-naphthaldehyde-N-methylpropanesulfonylhydrazone* were performed with the Gaussian 03W software package [38] by using DFT/B3LYP/6-311++G(d,p) method. All the parameters were allowed to relax, and all the calculations were converged to an optimized geometry which corresponds to a true energy minimum revealed by the lack of imaginary values in the wave numbers calculations. The  $^1\text{H}$  and  $^{13}\text{C}$  NMR chemical shifts of the compounds were calculated using the GIAO/B3LYP/6-311++G(d,p) method in  $\text{CDCl}_3$  solution.

#### Descriptor calculation

Geometry optimization of the Ni(II) complexes was performed by using DFT/B3LYP/6-31G(d,p) method in vacuum with Gaussian 03 software [38]. Gaussian outputs were loaded into CODESSA (version 2.7.10) software to calculate molecular descriptors.

#### Data sets

Antibacterial activity values of 33 Ni(II) sulfonyl hydrazone complexes synthesized in our laboratory previously [14,18,21,23,39], were screened against *S. aureus* and *E. coli* and used for QSAR (Table 4). Antimicrobial activity data were expressed in pMIC ( $-\log \text{MIC}$ ) and used as dependent variables in

**Fig. 2.** Molecular structure (a) and the crystal packing (b) of the *nafpsmh*.



regression analysis (Table 5). Data set was randomly divided into two sets: (a) training set (25 complexes) used for model development and, (b) test set (remaining 8 complexes) used for external validation.

#### Regression analysis

Best Multiple Linear Regression (BMLR) method embedded in CODESSA software was used to obtain the QSAR models. To validate the predictive capability of the models, the squared correlation coefficient ( $R^2$ ), leave-one-out cross-validated squared correlation coefficient ( $R^2_{cv}$ ), the Fisher criteria ( $F$ ), and standard error ( $s^2$ ) were used [40]. High  $R^2$  values, small standard deviations, high  $F$  values and high cross-validated squared correlation coefficient indicate the robustness of generated models. External validation was also used to perform a further check on the predictive capabilities of the models obtained from the training set.

## Results and discussion

### Structure of the compounds

#### X-ray spectrum

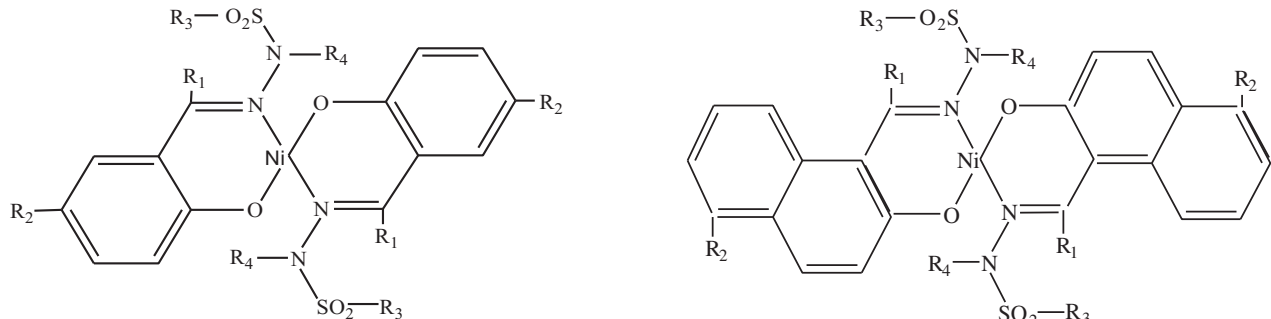
Unequivocal solid-state structure was confirmed through X-ray diffraction analyses of 2-hydroxy-1-naphthaldehyde-N-methylpropanesulfonylhydrazone whose ORTEP and Mercury diagrams are depicted in Fig. 2. There is an intramolecular hydrogen bond between the phenolic OH group and the iminic nitrogen, as evidenced by short O...N distances (Table 3). Thus, the length of the

C—O bond is 1.339 Å, which is consistent with a single bond; while the C=N bond distance is 1.284 Å. The mean plane of the heterocyclic ring is approximately coplanar with the naphthylmethylene fragment. The geometry around S1 atom is significantly deviated from that of regular tetrahedral. The maximum and minimum angles around S1 are 118.9(3)° and 104.8(3)°, respectively. In all essential details, the geometry of the molecule regarding bond lengths and angles of the compound are in good agreement with the values observed in similar structures [23,41]. Unit cell content indicating the crystal structure of the molecule is given in Fig. 2b.

#### IR spectra

The important IR spectral bands of the compounds along with their tentative assignments are given in Table 6. In the IR spectrum of the propanesulfonic acid 1-methylhydrazide, strong bands observed at 3340, 3251 and 1644  $\text{cm}^{-1}$  are assigned to the  $\nu_{as}(\text{NH}_2)$ ,  $\nu_s(\text{NH}_2)$  and  $\delta(\text{NH}_2)$  modes, respectively. Shifting of the  $\nu$  (C=N) frequency at 1621  $\text{cm}^{-1}$  of the 2-hydroxy-1-naphthaldehyde-N-methylpropanesulfonylhydrazone to a lower frequency by 15–25  $\text{cm}^{-1}$  (1596–1606  $\text{cm}^{-1}$ ) in all of its metal complexes (Table 6) is the evidence of the nitrogen bonding of the (C=N) group to the central metal atom. Shifting of the (C=O) stretching frequency at 1248  $\text{cm}^{-1}$  to a higher frequency by 39–58  $\text{cm}^{-1}$  (1287–1306  $\text{cm}^{-1}$ ) in the complexes is also an evidence of the oxygen bonding of the (C=O) group to the metal atom. This is further confirmed by the appearance of the new band at 555–570  $\text{cm}^{-1}$  due to (M—O) stretching modes of the metal complexes. In the IR spectra of 2-hydroxy-1-naphthaldehyde-N-methylpropanesulfonylhydrazone,

**Table 4**  
Structures of Ni(II) sulfonylhydrazone complexes used for datasets.



Comp.	R <sub>1</sub>	R <sub>2</sub>	R <sub>3</sub>	R <sub>4</sub>	Comp.	R <sub>1</sub>	R <sub>2</sub>	R <sub>3</sub>	R <sub>4</sub>
1	H—	H—	CH <sub>3</sub> —	H—	3	H—	H—	CH <sub>3</sub> —	H—
2	CH <sub>3</sub> —	H—	CH <sub>3</sub> —	H—	6	H—	5—CH <sub>3</sub> —	CH <sub>3</sub> —	H—
4	H—	p-CH <sub>3</sub> —	CH <sub>3</sub> —	H—	9	H—	H—	C <sub>2</sub> H <sub>5</sub> —	H—
5	CH <sub>3</sub> —	p-CH <sub>3</sub> —	CH <sub>3</sub> —	H—	12	H—	5—CH <sub>3</sub> —	C <sub>2</sub> H <sub>5</sub> —	H—
7	H—	H—	C <sub>2</sub> H <sub>5</sub> —	H—	15	H—	H—	C <sub>3</sub> H <sub>7</sub> —	H—
8	CH <sub>3</sub> —	H—	C <sub>2</sub> H <sub>5</sub> —	H—	18	H—	5—CH <sub>3</sub> —	C <sub>3</sub> H <sub>7</sub> —	H—
10	H—	p-CH <sub>3</sub> —	C <sub>2</sub> H <sub>5</sub> —	H—	21	H—	H—	C <sub>6</sub> H <sub>5</sub> —	H—
11	CH <sub>3</sub> —	p-CH <sub>3</sub> —	C <sub>2</sub> H <sub>5</sub> —	H—	24	H—	H—	C <sub>6</sub> H <sub>5</sub> —	CH <sub>3</sub> —
13	H—	H—	C <sub>3</sub> H <sub>7</sub> —	H—	27	H—	H—	CH <sub>3</sub> —	CH <sub>3</sub> —
14	CH <sub>3</sub> —	H—	C <sub>3</sub> H <sub>7</sub> —	H—	30	H—	H—	C <sub>2</sub> H <sub>5</sub> —	CH <sub>3</sub> —
16	H—	p-CH <sub>3</sub> —	C <sub>3</sub> H <sub>7</sub> —	H—	33	H—	H—	C <sub>3</sub> H <sub>7</sub> —	CH <sub>3</sub> —
17	CH <sub>3</sub> —	p-CH <sub>3</sub> —	C <sub>3</sub> H <sub>7</sub> —	H—					
19	H—	H—	C <sub>6</sub> H <sub>5</sub> —	H—					
20	CH <sub>3</sub> —	H—	C <sub>6</sub> H <sub>5</sub> —	H—					
22	H—	p-CH <sub>3</sub> —	C <sub>6</sub> H <sub>5</sub> —	CH <sub>3</sub> —					
23	CH <sub>3</sub> —	p-CH <sub>3</sub> —	C <sub>6</sub> H <sub>5</sub> —	CH <sub>3</sub> —					
25	H—	H—	CH <sub>3</sub> —	CH <sub>3</sub> —					
26	CH <sub>3</sub> —	H—	CH <sub>3</sub> —	CH <sub>3</sub> —					
28	H—	H—	C <sub>2</sub> H <sub>5</sub> —	CH <sub>3</sub> —					
29	CH <sub>3</sub> —	H—	C <sub>2</sub> H <sub>5</sub> —	CH <sub>3</sub> —					
31	H—	H—	C <sub>3</sub> H <sub>7</sub> —	CH <sub>3</sub> —					
32	CH <sub>3</sub> —	H—	C <sub>3</sub> H <sub>7</sub> —	CH <sub>3</sub> —					

**Table 5**  
Observed and predicted pMIC values and their difference for *S. aureus* and *E. coli*.

Comp.	<i>S. aureus</i>				<i>E. coli</i>			
	MIC (µg/mL)	Predicted	Observed	Difference	MIC (µg/mL)	Predicted	Observed	Difference
1	300	3.2111	3.2090	0.0021	225	3.1885	3.3380	-0.1495
2	395	3.1322	3.1140	0.0182	275	3.3096	3.2710	0.0386
3	250	3.3715	3.3700	0.0015	200	3.4876	3.4460	0.0416
4	280	3.2517	3.2630	-0.0113	325	3.3453	3.2000	0.1453
5	384	3.1542	3.1490	0.0052	305	3.4986	3.2500	0.2486
6	225	3.4264	3.4350	-0.0086	300	3.3021	3.3120	-0.0099
7	325	3.1809	3.1980	-0.0171	275	3.2236	3.2710	-0.0474
8	410	3.1428	3.1210	0.0218	300	3.3143	3.2560	0.0583
9	275	3.3617	3.3480	0.0137	250	3.4698	3.3890	0.0808
10	325	3.1857	3.2230	-0.0373	370	3.1869	3.1650	0.0219
11	325	3.1813	3.2430	-0.0617	392	3.3308	3.1620	0.1688
12	250	3.3794	3.4090	-0.0296	450	3.0609	3.1550	-0.0941
13	540	2.9222	3.0000	-0.0778	160	3.3622	3.5240	-0.1618
14	570	2.9798	3.0000	-0.0202	285	3.1588	3.3010	-0.1422
15	450	3.1991	3.1540	0.0451	270	3.5052	3.3760	0.1292
16	625	3.0323	2.9590	0.0733	225	3.3130	3.3970	-0.0840
17	657	3.0334	2.9580	0.0754	358	3.1028	3.2220	-0.1192
18	400	3.2280	3.2230	0.0050	250	3.4783	3.4280	0.0503
19	550	2.9833	3.0440	-0.0607	300	3.4991	3.3080	0.1911
20	600	3.1179	3.0260	0.0919	350	3.1634	3.2600	-0.0966
21	500	3.1171	3.1520	-0.0349	300	4.6905	4.9000	-0.2095
22	500	3.1069	3.1240	-0.0171	280	3.3532	3.3760	-0.0228
23	575	3.0417	3.0810	-0.0393	320	3.2729	3.2050	0.0679
24	450	3.2215	3.2140	0.0075	250	3.5219	3.4700	0.0519
25	600	2.9871	2.9320	0.0551	320	3.0480	3.2050	-0.1570
26	650	3.0102	2.9200	0.0902	1030	2.6418	2.7200	-0.0782
27	550	3.1650	3.0470	0.1180	753	2.9242	2.9110	0.0132
28	650	2.9059	2.9200	-0.0141	350	3.0340	3.1890	-0.1550
29	750	2.8637	2.8800	-0.0163	805	2.9209	2.8500	0.0709
30	600	3.1472	3.0290	0.1182	2380	2.6809	2.4300	0.2509
31	700	2.8130	2.9100	-0.0970	400	3.0597	3.1530	-0.0933
32	750	2.8218	2.9010	-0.0792	2370	2.6653	2.4010	0.2643
33	650	3.0541	3.0130	0.0411	2570	2.5427	2.4160	0.1267

**Table 6**  
Characteristic IR bands (cm<sup>-1</sup>) of the compounds.

Compounds	$\nu(\text{C-H})_{\text{ar}}$	$\nu_{\text{S}}(\text{SO}_2)$	$\nu_{\text{as}}(\text{SO}_2)$	$\nu(\text{C-O})$	$\nu(\text{C=C})$	$\nu(\text{C=N})$
psmh	–	1145s	1331s	–	–	–
nafpsmh	3069m	1142s	1334s	1248s	1576m	1621s
Cu(nafpsmh) <sub>2</sub>	2921m	1149s	1331s	1299m	1575m	1606s
Ni(nafpsmh) <sub>2</sub>	2928m	1147s	1329s	1306m	1568m	1596s
Pt(nafpsmh) <sub>2</sub>	2933m	1149s	1335s	1303w	1572m	1601s
Pd(nafpsmh) <sub>2</sub>	2925m	1144s	1327s	1287w	1575m	1600s

vibrational band observed at 1142 and 1334 cm<sup>-1</sup> are assigned to asymmetric and symmetric SO<sub>2</sub> stretching modes, respectively. Not shifting of symmetric and asymmetric SO<sub>2</sub> modes in the complexes is attributed to not participating in coordination.

#### NMR spectra

H and C atom shielding tensors were calculated using GIAO/B3LYP/6-311G++(d,p) method in CDCl<sub>3</sub> solution in order to facilitate the interpretation of the NMR spectra of *propanesulfonic acid 1-methylhydrazide* and *2-Hydroxy-1-naphthaldehyde-N-methylpropanesulfonylhydrazone*. The DEPT spectrum of *2-hydroxy-1-naphthaldehyde-N-methylpropanesulfonylhydrazone* is given in Fig. 3. Most of the experimental and calculated chemical shift values (in Table 7) showed good agreement to each other. However, the NH<sub>2</sub> and HO peaks were observed at 4.6 ppm, and 11.84 ppm in the NMR spectrum, and calculated as 3.98 ppm and 10.92 ppm respectively. These discrepancies are attributed to existence of intramolecular hydrogen bonding between OH and CN group. The singlet peak belonging to the azomethine CH=N proton at 8.67 ppm indicates the predominance of the phenolic-imine tautomer in the *2-hydroxy-1-naphthaldehyde-N-methylpropanesulfonylhydrazone* [23,42].

The molar conductivity ( $\Lambda_m$ ) of 10<sup>-3</sup> M solutions of the complexes in DMF at 25 °C were measured, and all the complexes were found to be of non-electrolytic nature in the range of 11–19 Ω<sup>-1</sup>·cm<sup>2</sup> mol<sup>-1</sup> [20]. The room temperature magnetic moment of the copper(II) complex was found to be 1.76 B.M. Magnetic moment, MS-molecular ion peak values and molar conductivity values suggest a four-coordinate structure in the solid state for Cu(II) complex [43,44]. The diamagnetic character of the nickel(II), platinum(II) and palladium(II) complexes implies square-planar stereochemistry for these complexes.

#### Antibacterial activity

Antibacterial activity of the compounds and reference drugs (Ciprofloxacin and Ampicillin) were screened in vitro against three Gram-positive species (*S. aureus*, *B. subtilis*, and *B. cereus*) and three Gram-negative species (*E. coli*, *P. aeruginosa* and *Y. enterocolitica*) by using microdilution and disc diffusion methods. Antibacterial activity values were tabulated in Tables 8 and 9.

Our compounds showed a broad spectrum of activity against tested bacteria. They showed better antibacterial activity against Gram-negative bacteria. According to disc diffusion data, *psmh*, *Pt(nafpsmh)<sub>2</sub>* and *Pd(nafpsmh)<sub>2</sub>* exhibited the significant activity against Gram-negative bacteria (~23–19 mm) whereas *Cu(nafpsmh)<sub>2</sub>* showed moderate activity (17–19 mm), and *Ni(nafpsmh)<sub>2</sub>* showed the lowest activity against all bacteria (9–11 mm). Reference drugs showed better activity than our compounds in all tested strains.

It will be important to choose the concentration unit to express activity order. Depending on the units of concentration, activity order of compounds would be different. For example, if you choose the µg/mL, activity order will be as following:

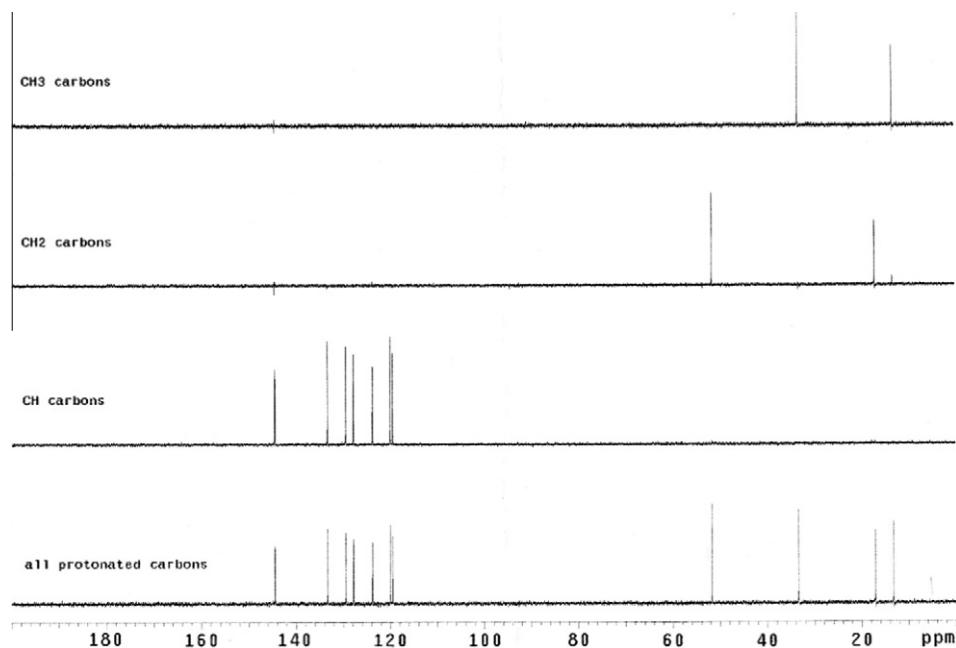


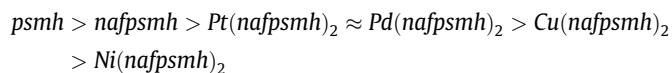
Fig. 3. DEPT spectrum of the *nafpsmh*.

Table 7

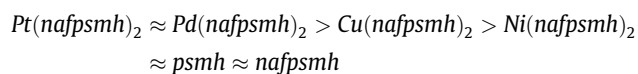
The experimental and theoretical  $^1\text{H}$  and  $^{13}\text{C}$  NMR chemical shifts  $\delta(\text{ppm})$  of the *psmh* and *nafpsmh*.

Assignment	<i>psmh</i>		<i>nafpsmh</i>	
	$\delta(\text{exp.})$	$\delta(\text{calc.})^a$	$\delta(\text{exp.})$	$\delta(\text{calc.})^a$
C-1	–	–	120.00	118.45
C-2	–	–	129.43	128.19
C-3	–	–	123.81	123.38
C-4	–	–	128.45	129.93
C-5	–	–	127.82	128.18
C-6	–	–	132.25	132.28
C-7	–	–	108.32	108.51
C-8	–	–	158.47	158.67
C-9	–	–	119.48	118.44
C-10	–	–	133.30	133.86
C-11	–	–	144.45	138.86
C-12	33.40	38.14	33.33	27.19
C-13	53.80	57.36	51.70	59.33
C-14	17.38	20.13	17.02	20.18
C-15	13.15	12.45	13.23	12.00
H-1	–	–	8.67(s, H)	8.21
H-2	–	–	7.52(t, H)	7.85
H-3	–	–	7.37(t, H)	7.63
H-4	–	–	7.67(d, H)	8.03
H-9	–	–	7.17(d, H)	7.43
H-10	–	–	7.97(d, H)	8.19
H-11	–	–	8.67(s, H)	8.54
H-12	2.90(s, 3H)	2.80	3.43(s, 3H)	3.35
H-13	3.15(m, 2H)	3.07	3.13(m, 2H)	3.54
H-14	1.49(m, 2H)	1.75	1.87(m, 2H)	1.81
H-15	0.98(t, 3H)	1.14	1.04(t, 3H)	1.22
OH	–	–	11.84	10.92
NH <sub>2</sub>	4.6	3.98	–	–

<sup>a</sup> Calculated using GIAO/ B3LYP/6-31++G(d,p) method in CDCl<sub>3</sub>.



However, if you use mM units, the order above would change as following:



According to MIC values in molar units, *Pt(nafpsmh)*<sub>2</sub> and *Pd(nafpsmh)*<sub>2</sub> complexes showed the best activity against all bacteria (0.093–0.208 mM). *Cu(nafpsmh)*<sub>2</sub> exhibited moderate activity against all bacteria (0.222 mM). *psmh* exhibited the best activity against *Y. enterocolitica* 0:3 at a concentration of 37.5 μg/mL (0.244 mM) but *nafpsmh* showed the best activity against *E. coli* ATCC 35218 at a concentration of 75 μg/mL (0.244 mM).

Generally, Pt(II) and Pd(II) complexes are more active than Cu(II) and Ni(II) complexes. However, it is proved to be more beneficial against several diseases to use low molecular weight complexes [45] and therefore, we prefer to use Ni(II) complexes to investigate the structure–activity relationship.

#### QSAR analysis

Structures of 33 Ni(II) sulfonyl hydrazones used in regression analysis were given in Table 8. Observed and predicted pMIC values and their difference for *S. aureus* ATCC 25923 and *E. coli* ATCC 25922 were listed in Table 5. To select the optimum number of descriptors for QSAR analysis, the “breaking point” rule was applied, hence, squared correlation coefficient  $R^2$  values of training set was plotted as a function of descriptor numbers (Fig. 4). In this diagram, descriptor number corresponding to the breaking point is considered the best/optimum model. Consequently, four descriptors were used as independent variables in our models. Four-parameter QSAR equations obtained by using BMLR method, were given in Table 10. In Table 10, X and  $\Delta X$  stand for the regression coefficient values and their standard errors for each of the descriptors, while the *t*-test represents the significance of the descriptors within the equation. More is the value, more is the significance. A graphical presentation of the relationship between the experimental and the predicted pMIC values for training sets were given in Fig. 5. Statistical validation of the models demonstrated that the proposed model has a normal statistical stability and validity. The absence of colinearity among the used descriptors is confirmed by intercorrelation matrix for the independent variables used in our models (Table 11). No significant correlation was found among the descriptors which were in the same equation. In order to confirm

**Table 8**  
Measured inhibition zone diameter of the compounds and antibiotics by disc diffusion method.

Bacteria strains	Diameter inhibition zone (mm, 200 µg/disk)							
	<i>psmh</i>	<i>nafpsmh</i>	Ni ( <i>nafpsmh</i> ) <sub>2</sub>	Cu( <i>nafpsmh</i> ) <sub>2</sub>	Pt ( <i>nafpsmh</i> ) <sub>2</sub>	Pd( <i>nafpsmh</i> ) <sub>2</sub>	SD <sup>a</sup>	SD <sup>b</sup>
<i>Gram-negative</i>								
<i>E. coli</i> ATCC 35218	22	18	10	19	22	20	12	37
<i>P. aeruginosa</i> ATCC 27853	20	17	11	18	20	19	10	–
<i>Y. enterocolitica</i> 0:3	23	20	11	17	20	19	9	–
<i>Gram-positive</i>								
<i>B. cereus</i> RSKK 709	17	14	10	14	17	16	13	25
<i>B. subtilis</i> ATCC 6633	17	12	9	10	16	15	11	–
<i>S. aureus</i> ATCC 25923	18	14	10	11	18	15	17	29

<sup>a</sup> Ampicillin (10 µg/disk).

<sup>b</sup> Ciprofloxacin (5 µg/disk) < 10: weak; >10 moderate; >16: significant.

**Table 9**  
The MIC values of antibacterial activity of the compounds.

Bacteria strains	MIC µg mL <sup>-1</sup> (mM)					
	<i>psmh</i>	<i>nafpsmh</i>	Ni ( <i>nafpsmh</i> ) <sub>2</sub>	Cu( <i>nafpsmh</i> ) <sub>2</sub>	Pt ( <i>nafpsmh</i> ) <sub>2</sub>	Pd ( <i>nafpsmh</i> ) <sub>2</sub>
<i>Gram-negative</i>						
<i>E. coli</i> ATCC 35218	37.5 ( <b>0.247</b> )	75 ( <b>0.244</b> )	300 ( <b>0.448</b> )	150 ( <b>0.222</b> )	75 ( <b>0.093</b> )	150 ( <b>0.208</b> )
<i>P. aeruginosa</i> ATCC 27853	75 ( <b>0.492</b> )	150 ( <b>0.489</b> )	150 ( <b>0.224</b> )	150 ( <b>0.222</b> )	75 ( <b>0.093</b> )	75 ( <b>0.104</b> )
<i>Y. enterocolitica</i> 0:3	37.5 ( <b>0.242</b> )	150 ( <b>0.489</b> )	150 ( <b>0.224</b> )	150 ( <b>0.222</b> )	150 ( <b>0.186</b> )	75 ( <b>0.104</b> )
<i>Gram-positive</i>						
<i>B. cereus</i> RSKK 709	75 ( <b>0.492</b> )	150 ( <b>0.489</b> )	300 ( <b>0.448</b> )	150 ( <b>0.222</b> )	75 ( <b>0.093</b> )	75 ( <b>0.104</b> )
<i>B. subtilis</i> ATCC 6633	75 ( <b>0.492</b> )	150 ( <b>0.489</b> )	300 ( <b>0.448</b> )	150 ( <b>0.222</b> )	75 ( <b>0.093</b> )	75 ( <b>0.104</b> )
<i>S. aureus</i> ATCC 25923	75 ( <b>0.492</b> )	150 ( <b>0.489</b> )	150 ( <b>0.224</b> )	300 ( <b>0.444</b> )	150 ( <b>0.186</b> )	150 ( <b>0.208</b> )

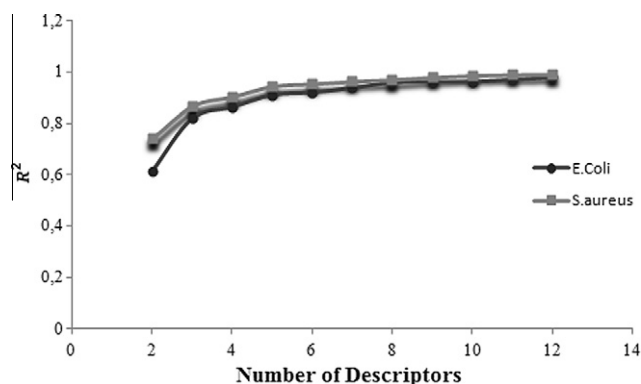


**Fig. 4.**  $R^2$  values versus the number of descriptors used for the models.

the QSAR equations, antimicrobial activity values of compounds in the test set were predicted by using obtained equations. A graphical presentation of the relationship between the experimental and the predicted pMIC values for test sets were given in Fig. 6. Observed and predicted values are very close to each other. The test set has an acceptable external correlation coefficient ( $r^2 > 0.85$ ).

In evaluation of the regression equations in QSAR model for *S. aureus*, nucleophilic reactivity index for a Ni atom which is defined as follows [46] plays an important role in anti-bacterial activities of Ni(II) sulfonyl hydrazones.

$$N_A = \sum_{i \in A} C_{iHOMO}^2 / (1 - \epsilon_{HOMO})$$

This equation shows that the energies of HOMO affect the activity. It is well-known that HOMO is responsible for the formation of charge transfer in a chemical reaction and characterizes the susceptibility of the molecule towards to electrophiles. The negative coefficient of it indicates that the lower the nucleophilic reactivity index, the greater the anti-microbial activity. The second impor-

tant parameter is the HOMO–LUMO energy gap which is related to polarizability, softness and charge migration during the enzyme–drug interaction. As the HOMO–LUMO energy gap decreased, softness and anti-bacterial activity of the compounds increased. The third descriptor, hydrogen bond acceptor dependent hydrogen bond donor surface area (HDCA-2) is an electrostatic parameter representing the hydrogen bonding acceptor properties of the compounds. Its positive sign suggests that the most effective compounds act mainly as hydrogen-bonding acceptors. According to its “t-value,” the least significant descriptor in the model is average valency of an S atom. Its negative sign suggests that when the average valency of an S atom decreases, the antibacterial activity increases.

The first descriptor in the QSAR model for *E. coli* is “nucleophilic reaction index for an O atom”. Positive sign for the coefficient of this descriptor indicates that the increase in nucleophilic reaction index for an O atom of these molecules causes increase in the anti-bacterial activity. The third descriptor “DPSA-1” is equal to difference between partial positively and negatively charged surface areas [47,48]. It is directly related to electrostatic interactions, and indirectly related to the hydrogen bonding ability of a molecule. The positive regression coefficient for this descriptor reflects the fact that the larger value of this descriptor leads to higher binding ability. The least significant descriptor is “average bond order of an O atom” [49]. Its positive coefficient indicates that activity of the compounds increases when the average bond order of an O atom increases.

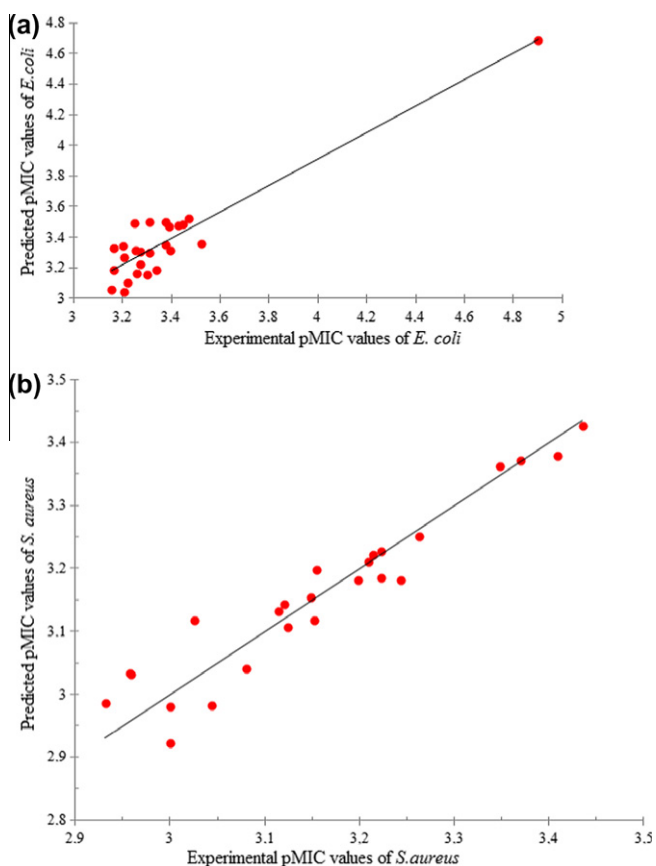
From the model equations, we can predict that nucleophilic reaction index for Ni and O atom affect the antimicrobial activity of Ni(II) sulfonylhydrazone complexes, and HOMO–LUMO energy gap is the second important parameter for activity. When the energy gap decreased, softness and anti-bacterial activity of the compounds increased. In addition, hydrogen bonding acceptor properties of the compounds is also an important parameter.



**Table 10**

Four-parameter QSAR models by using BMLR method.

	No	X	$\pm\Delta X$	t-test	Descriptors
<i>S. aureus</i>					
Training set	0	0.8480e-01	9.2571e-02	1.4779	Intercept
$R^2 = 0.9046$	1	-3.2345e+01	3.1905e-01	-10.3693	Nucleoph.react.index for a Ni atom
$R^2_{cv} = 0.8517$	2	-1.8332e+01	1.7481e-01	-10.2272	HOMO-LUMO energy gap
$F = 47.39$	3	9.6249e-01	1.2238e-01	6.8647	HA dependent HDCA-2
$s^2 = 0.0023$	4	-1.3327e-01	1.7964e-02	-4.6386	Avg valency of a S atom
Test set					
$R^2 = 0.8550$					
<i>E. coli</i>					
Training set	0	-6.3441e-03	1.2046e-04	-1.2667	Intercept
$R^2 = 0.8635$	1	5.1298e+02	4.5743e-03	9.0282	Nucleoph. react. index for a O atom
$R^2_{cv} = 0.4318$	2	-4.0989e+02	3.3683e-03	-9.4981	HOMO-LUMO energy gap
$F = 31.63$	3	3.0655e+01	2.4012e+00	5.0730	DPSA-1
$s^2 = 0.0184$	4	2.1472e+01	1.5170e+00	3.3705	Avg bond order of a O atom
Test set					
$R^2 = 0.8693$					

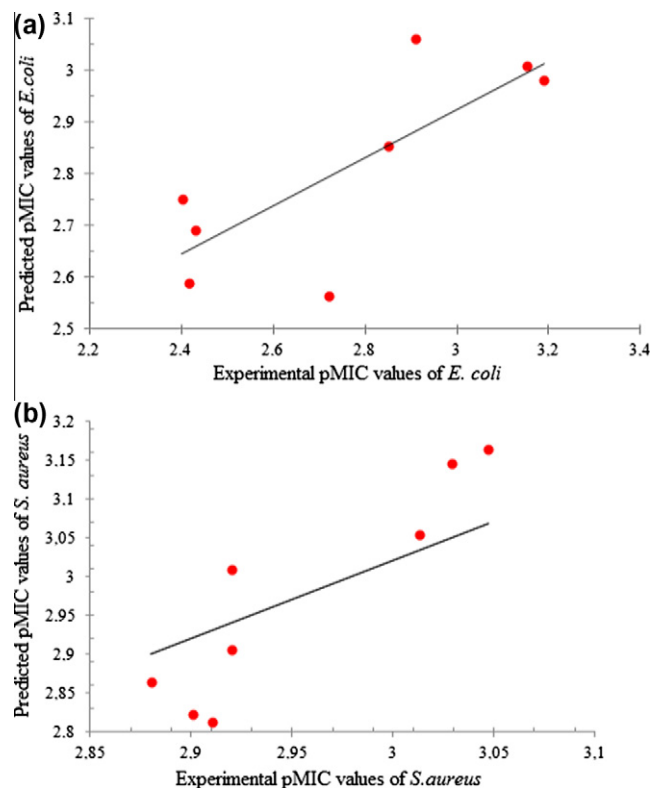
**Fig. 5.** Plot of observed versus calculated pMIC values of training sets for: (a) *E. coli* and (b) *S. aureus*.

## Conclusion

Obtained results demonstrate that Pt(II) and Pd(II) sulfonylhydrazone complexes showed the best antimicrobial activities against all bacteria. 2D-QSAR analysis for *E. coli* and *S. aureus* were performed on 33 Ni(II) complexes by using BMLR method. According to the four-descriptor QSAR model, nucleophilic reactivity index for a Ni atom, HOMO-LUMO energy gap, HDCA-2 and average valency of an S atom were the effective descriptors for *S. aureus*. As the HOMO-LUMO energy gap and nucleophilic reactivity index decreases, anti-bacterial activities increase; viz. softness of

**Table 11**Intercorrelation matrix of the descriptors used in *S. aureus* and *E. coli*.

For <i>S. aureus</i>	$\Delta E$	AVS	HDCA-2	MVH
$\Delta E$	1.0000	-0.0676	-0.0020	-0.4514
AVS		1.0000	0.5030	-0.3173
HDCA-2			1.0000	-0.2426
MVH				1.0000
For <i>E. coli</i>	ABOO	DPSA-1	MNRIO	ZX
ABOO	1.0000	-0.3871	-0.5067	-0.2827
DPSA-1		1.0000	0.3165	0.3447
MNRIO			1.0000	-0.4010
ZX				1.0000

**Fig. 6.** Plot of observed versus calculated pMIC values of test sets for: (a) *E. coli* and (b) *S. aureus*.

molecules increases the activity, namely, as seen in soft Pt and Pd complexes. In addition, increasing hydrogen bonding acceptor properties of the compounds will increase electrostatic interaction and antibacterial activity as well.

For *E. coli.*, nucleophilic reaction index for O atom, HOMO–LUMO energy gap, DPSA-1 and average bond order of an O atom play a key role in the antimicrobial activity. Accordingly, charge distribution or relative reactivity of the oxygen atoms in the molecules affects the antimicrobial activity, in other words, factors that increase negative charge on O atom also increase the activity. Decrease in HOMO–LUMO energy gap, second important parameter; imply that soft molecules will have higher antimicrobial activities. In addition, electrostatic interaction ability of the compounds will influence the activity, for example, increasing difference between positive and negative charge on surface area of the molecule, that is polarity, increases the antimicrobial activity. Briefly, compounds that are more polar, soft and with more electronegative O atoms and hydrogen bonding acceptor sites will have higher antimicrobial activity.

### Acknowledgement

The authors would like to thank Gazi University BAP (Grant No: 05/2010-43) for the financial support of this project.

### References

- [1] G. Domagk, Deut. Med. Wochenschr. 61 (1935) 250–253.
- [2] P.B. Molinoff, R.W. Ruddon, A.G. Gilman, Goodman's and Gilman's the Pharmacological Basis of Therapeutics, ninth ed., McGraw-Hill, New York, 1996.
- [3] A.O. Carl, S.M. Couchman, J.C. Jeffery, K.L.V. Mann, E. Psillakis, M.D. Ward Inorg. Chim. Acta 278 (1998) 178–184.
- [4] M. Zheng, C. Xu, J. Ma, Y. Sun, F. Du, H. Liu, L. Lin, C. Li, J. Ding, K. Chena, H. Jianga, Bioorg. Med. Chem. 15 (2007) 1815–1827.
- [5] M.M. Kamel, H.I. Ali, M.M. Anwar, N.A. Mohamed, A.M. Soliman, Eur. J. Med. Chem. 45 (2010) 572–580.
- [6] M. Ferraroni, F. Briganti, W.R. Chegwiddden, C.T. Supuran, A. Scozzafava, Inorg. Chim. Acta 339 (2002) 135–144.
- [7] N. Siddiqui, M.F. Arshad, S.A. Khan, W. Ahsan, J. Enzyme Inhib. Med. Chem. 25 (2010) 485–491.
- [8] M. Bülbül, R. Kasımoğulları, Ö. Küfrevioğulları, J. Enzyme. Inhib. Med. Chem. 23 (2008) 895–900.
- [9] M. Jaiswal, P.V. Khadikara, C.T. Supuran, Bioorg. Med. Chem. Lett. 14 (2004) 5661–5666.
- [10] C.W. Thornber, Chem. Soc. Rev. 8 (1979) 563–580.
- [11] A.Ç. Scozzafava, T. Owa, A. Mastrolorenzo, C.T. Supuran, Curr. Med. Chem. 10 (2003) 925–953.
- [12] R. Rönn, Y.A. Sabnis, T. Gossas, E.A. Kerblom, H. Danielson, A. Hallberga, A. Johanssona, Bioorg. Med. Chem. 14 (2006) 544–559.
- [13] Ü.Ö. Özdemir, F. Aslan, F. Hamurcu, Spectrochim. Acta Part A 75 (2010) 121–126.
- [14] Ü. Özdemir, P. Güvenç, E. Şahin, F. Hamurcu, Inorg. Chim. Acta 362 (2009) 2613–2618.
- [15] G. Alzuet, J. Borras, F. Estevan, M. Liu-Gonzalez, F. Sanz-Ruiz, Inorg. Chim. Acta 343 (2003) 56–60.
- [16] P.A. Aijbade, G.A. Kolawole, P. O'Brien, M. Helliwell, J. Raftery, Inorg. Chim. Acta 359 (2006) 3111–3116.
- [17] Z.H. Chohan, H.A. Shad, M.H. Youssoufi, T.B. Hadda, Eur. J. Med. Chem. 45 (2010) 2893–2901.
- [18] Ü.Ö. Özmen, G. Olgun, Spectrochim. Acta Part A 70 (2009) 641–645.
- [19] H.C. Zahid, H.A. Shad, J. Enzyme. Inhib. Med. Chem. 23 (2008) 369–376.
- [20] Z.H. Chohan, A.U. Shaikh, M.M. Naseer, C.T. Supuran, J. Enzyme. Inhib. Med. Chem. 21 (2006) 771–781.
- [21] N.I. Dodoff, Ü. Özdemir, N. Karacan, M. Georgieva, S.M. Konstantinov, M.E. Stefanova, Z. Naturforsch. 54 (1999) 1553–1562.
- [22] N. Özbek, S. Alyar, N. Karacan, J. Mol. Struct. 938 (2009) 48–53.
- [23] N. Özbek, G. Kavak, Y. Özcan, S. İde, N. Karacan, J. Mol. Struct. 919 (2009) 154–159.
- [24] S. Alyar, H. Zengin, N. Özbek, N. Karacan, J. Mol. Struct. 992 (2011) 27–32.
- [25] N. Özbek, S. Alyar, S. Mamaş, E. Şahin, N. Karacan, J. Mol. Struct. 1010 (2012) 1–7.
- [26] V.X. Siew, I. tan, J.D. Ranford, Inorg. Chim. Acta 358 (2005) 677–686.
- [27] R. Kumar, P. Kumar, M. Kumar, B. Narasimhan, Med. Chem. Res. 21 (2012) 4301–4310.
- [28] D. Mandloi, S. Joshi, P.V. Khadikar, N. Khosla, Bioorg. Med. Chem. 15 (2005) 405–411.
- [29] A.A.M. Abdel-Aziz, Y.A. Asiri, H.M. Agamy, Eur. J. Med. Chem. 46 (2011) 5487–5497.
- [30] R. Dhondge, S.C. Chaturvedi, Med. Chem. Res. 18 (2009) 167–178.
- [31] K.K. Sahu, V. Ravichandran, V.K. Mourya, R.K. Agrawal, Med. Chem. Res. 15 (2007) 418–430.
- [32] C. Hansch, A. Leo, Exploring QSAR: Fundamentals and Applications in Chemistry and Biology, American Chemical Society, Washington, 1995.
- [33] S. Alyar, N. Özbek, K. Kuzukıran, N. Karacan, Med. Chem. Res. 20 (2011) 175–183.
- [34] Rigaku, CRYSTAL CLEAR, Version 1.3.6., Rigaku American Corporation 9009 New Trails Drive, The Woodlands, TX 77381-5209, USA, 2005.
- [35] G.H. Sheldrick, SHELXS-97 and SHELXL-97 University of Göttingen, Germany 1997.
- [36] A.W. Bauer, W.M. Kirby, J.C. Sherris, M. Turck, Am. J. Clin. Pathol. 45 (1966) 493–496.
- [37] G. Küçükgülzel, A. Kocatepe, E.D. Clercq, F. Şahin, M. Güllüce, Eur. J. Med. Chem. 41 (2006) 353–359.
- [38] M.J. Frisch, G.W. Trucks, H.B. Schlegel, G.E. Scuseria, M.A. Robb, J.R. Cheeseman, J.A. Montgomery, Jr., T. Vreven, K.N. Kudin, J.C. Burant, J.M. Millam, S.S. Iyengar, J. Tomasi, V. Barone, B. Mennucci, M. Cossi, G. Scalmani, N. Rega, G.A. Petersson, H. Nakatsuji, M. Hada, M. Ehara, K. Toyota, R. Fukuda, J. Hasegawa, M. Ishida, T. Nakajima, Y. Honda, O. Kitao, H. Nakai, M. Klene, X. Li, J.E. Knox, H.P. Hratchian, J.B. Cross, V. Bakken, C. Adamo, J. Jaramillo, R. Gomperts, R.E. Stratmann, O. Yazyev, A.J. Austin, R. Cammi, C. Pomelli, J.W. Ochterski, P.Y. Ayala, K. Morokuma, G.A. Voth, P. Salvador, J.J. Dannenberg, V.G. Zakrzewski, S. Dapprich, A. D. Daniels, M.C. Strain, O. Farkas, D.K. Malick, A.D. Rabuck, K. Raghavachari, J.B. Foresman, J.V. Ortiz, Q. Cui, A.G. Baboul, S. Clifford, J. Cioslowski, B.B. Stefanov, G. Liu, A. Liashenko, P. Piskorz, I. Komaromi, R.L. Martin, D.J. Fox, T. Keith, M.A. Al-Laham, C.Y. Peng, A. Nanayakkara, M. Challacombe, P.M.W. Gill, B. Johnson, W. Chen, M.W. Wong, C. Gonzalez, J. A. Pople, Gaussian, Inc., Wallingford CT, Gaussian 03, Revision C.02, Gaussian, Inc., C.T. Wallingford 2004.
- [39] O.S. Senturk, U. Ozdemir, S. Sert, N. Karacan, F. Ugur, J. Coord. Chem. 60 (2007) 229–235.
- [40] A. Katritsky, M. Karelson, V.S. Lobanov, R. Dennington, T. Keith, CODESSA 2.7.10., Semicem. Inc., Shawnee, KS 2004.
- [41] T. Hokelek, S. Bilge, S. Demiriz, B. Ozguc, Z. Kılıc, Acta Cryst. C60 (2004) 803–805.
- [42] N. Ancin, O. Celik, S.G. Öztas, S. Ide, Struct. Chem. 18 (2007) 347–352.
- [43] N. Raman, A. Kulandaisamy, A. Shunmugasundaram, K. Jeyasubramanian, Trans. Met. Chem. 26 (2001) 131–135.
- [44] C.A. Otter, S.M. Couchman, J.C. Jeffery, K.L.V. Mann, E. Psillids, M.D. Ward Inorg. Chim. Acta 278 (1998) 178.
- [45] S.E. Castillo-Blum, N. Barba-Behrens, Coord. Chem. Rev. 196 (2000) 3–30.
- [46] R. Franke, Theoretical Drug Design Methods, Elsevier, Amsterdam, 1984.
- [47] D.T. Stanton, P.C. Jurs, Anal. Chem. 62 (1990) 2323–2329.
- [48] D.T. Stanton, L.M. Ego, P.C. Jurs, M.G. Hicks, J. Chem. Inf. Comput. Sci. 32 (1992) 306–316.
- [49] A.B. Sannigrahi, Adv. Quant. Chem. 23 (1992) 301–351.